American Mineralogist, Volume 98, pages 2164–2171, 2013

New experimental data on phase relations for the system Na_2CO_3-$CaCO_3$ at 6 GPa and 900–1400 ºC

Anton Shatskiy[1,2,*], Igor S. Sharygin[1,2], Konstantin D. Litasov[1,2], Yuri M. Borzdov[1], Yuri N. Palyanov[1,2] and Eiji Ohtani[3]

[1]V.S. Sobolev Institute of Geology and Mineralogy, Russian Academy of Science, Siberian Branch, Koptyuga pr. 3, Novosibirsk 630090, Russia
[2]Novosibirsk State University, Novosibirsk 630090, Russia
[3]Department of Earth and Planetary Material Science, Tohoku University, Sendai 980-8578, Japan

Abstract

Phase relations in the system Na_2CO_3-$CaCO_3$ have been studied in the compositional range, $X(Na_2CO_3)$, from 100 to 10 mol%, at 6.0 GPa and 900–1400 °C. Below 1100 °C, the system has three intermediate compounds: $Na_4Ca(CO_3)_3$, $Na_2Ca_3(CO_3)_4$, and $Na_2Ca_4(CO_3)_5$. The $Na_4Ca(CO_3)_3$ and $Na_2Ca_3(CO_3)_4$ compounds melt congruently slightly above 1200 and 1300 °C, respectively. The eutectics were established at 70 and 52 mol% near 1200 °C and at 21 mol% near 1300 °C. The $Na_2Ca_4(CO_3)_5$ compound decomposes to the $Na_2Ca_3(CO_3)_4$ + aragonite assembly at 1100 °C. Maximum solid solution of $CaCO_3$ in Na_2CO_3 is 6–8 mol% at 1100–1300 °C. Melting of Na_2CO_3 occurs between 1350 and 1400 °C. Na solubility in aragonite does not exceed the detection limit (<0.5 mol%). Aragonite remains a liquidus phase at 1300 and 1400 °C.

Keywords: Na-Ca carbonate, high-pressure, aragonite, natrite, shortite, nyerereite, natrocarbonatite, Earth's mantle

Introduction

It has been shown that the presence of CO_2 substantially lowers the melting temperature of mantle rocks (Wyllie and Huang 1975; Dalton and Presnall 1998; Dasgupta and Hirschmann 2006; Litasov and Ohtani 2009, 2010; Dasgupta et al. 2013), and plays an essential role in mantle metasomatism (Green and Wallace 1988; Haggerty 1989; Yaxley et al. 1991; Walter et al. 2008) and diamond formation (Akaishi et al. 1990; Kanda et al. 1990; Pal'yanov et al. 1999, 2002; Shatskii et al. 2002; Palyanov et al. 2007). According to studies of the melt inclusions in diamonds (Navon 1991; Schrauder and Navon 1994; Klein-BenDavid et al. 2009; Weiss et al. 2009; Logvinova et al. 2011; Zedgenizov et al. 2011) and melting experiments (Wallace and Green 1988; Brey et al. 2011; Grassi and Schmidt 2011; Litasov et al. 2013), the specific feature of these melts is high alkali contents. It is, therefore, essential to know the phase relations in simple alkali-alkaline earth carbonate systems under mantle conditions.

As part of an investigation of those systems, Na_2CO_3-$CaCO_3$ is important, given the Na and Ca abundances in natrocarbonatite lavas (Dawson 1962; Hay 1983; Zaitsev and Keller 2006) and in the groundmass of fresh kimberlites (Watkinson and Chao 1973; Cooper and Gittins 1974; Kamenetsky et al. 2004, 2007). The given system is also important in view of the Na and Ca abundances in carbonatite melts entrapped by olivine and Cr-spinel from kimberlites (Kamenetsky et al. 2009, 2012), sheared peridotite xenoliths (190–220 km depth) (Korsakov et al. 2009; Golovin et al. 2012), and some "fibrous" diamonds (Klein-BenDavid et al. 2004, 2007; Kaminsky et al. 2009).

Although phase relations in alkali-earth carbonate systems were studied extensively from upper down to lower mantle conditions, e.g., (Ono et al. 2005, 2007; Buob et al. 2006; Merlini et al. 2012a, 2012b; Spivak et al. 2012), the studies of alkali-bearing carbonate systems and in particular the system Na_2CO_3-$CaCO_3$ (Fig. 1), were limited by 0.1 GPa (Eitel and Skaliks 1929; Cooper et al. 1975). In this study we extended an available pressure range for this system and studied phase relations at 6 GPa and 900–1400 °C.

Experimental methods

In this study we conducted multi-anvil experiments to constrain phase relations in the system Na_2CO_3-$CaCO_3$ using DIA- and wedge-type presses at Tohoku University (Sendai, Japan) (Shatskiy et al. 2011b) and BARS apparatus at V.S. Sobolev's IGM SB RAS (Novosibirsk, Russia) (Palyanov et al. 2010; Shatskiy et al. 2011a). All experiments were performed using graphite sample capsules, which are conventionally employed to seal alkali-carbonate melts in long duration experiments (up to 20–40 h) under 6.0 ± 0.5 GPa pressures and temperatures up to 1650 °C (Kanda et al. 1990; Shatskii et al. 2002). The experimental methods employed in the present study were the same as in our recent manuscript (Shatskiy et al. 2013). Here, we will only focus on peculiarities of measurement of chemical composition of carbonate phases in the Na_2CO_3-$CaCO_3$ system using energy-dispersive scanning electron microprobe.

Samples were studied using a JSM 5410 scanning electron microscope equipped with Oxford Instruments Link ISIS Series 300 energy-dispersive X-ray spectrometer (EDS) at Tohoku University (Sendai, Japan). The EDS spectra were collected by rastering the electron beam over a surface area available for the analysis with linear dimensions from 10 to 300 μm at 15 kV accelerating voltage and 10 nA beam current. The EDS was calibrated at the same conditions by rastering the electron beam over a sample cross-section area, up to 0.5–0.8 mm in linear dimensions. For that purpose, we employed post-experimental samples with known compositions and a homogeneous texture (i.e., samples that underwent complete melting and samples synthesized well below eutectic temperatures). We also

* E-mail: anton.antonshatskiy.shatskiy@gmail.com

0003-004X/13/1112–2164$05.00/DOI: http://dx.doi.org/10.2138/am.2013.4436

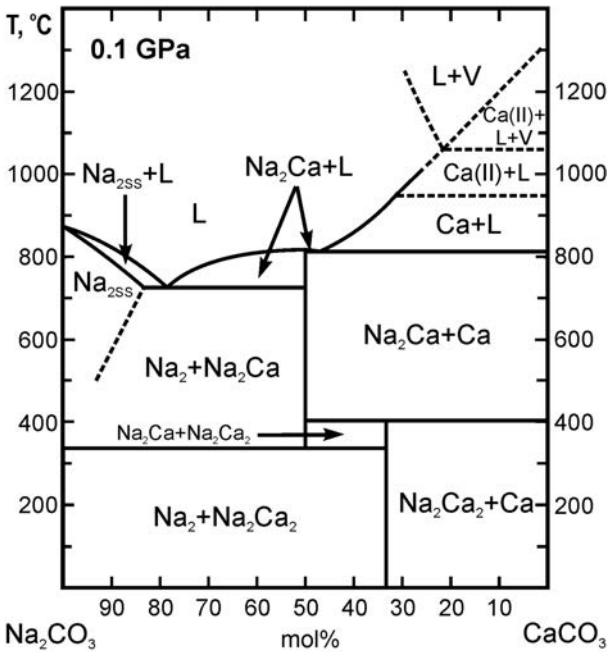

FIGURE 1. Phase relations in the system Na_2CO_3-$CaCO_3$ at 0.1 GPa, modified after Cooper et al. (1975). Na_2 = Na_2CO_3; Na_{2SS} = Na carbonate solid solutions; Na_2Ca = $Na_2Ca(CO_3)_2$ (nyerereite); Na_2Ca_2 = $Na_2Ca_2(CO_3)_3$ (shortite), Ca = calcite; Ca(II) = calcite II; L = liquid; V = vapor.

confirmed that the size of the analyzed region has no effect on the resulting data, as long as the area is significantly larger than the grain size. We found significant deficit of Na relative to the actual composition. The deficit systematically increases from the end-member sides (Na_2CO_3 and $CaCO_3$) toward the apparent compositions near 30–40 mol% Na_2CO_3. The results of calibration are shown in Figure 2. The best fit of the data is described by following polynomial expression: $k = 0.86671 + 0.02681 \times X - 7.63271 \times 10^{-4} \times X^2 + 8.60987 \times 10^{-6} \times X^3 - 3.55568 \times 10^{-8} \times X^4$, where X is the measured content of Na_2CO_3 and k is the correction factor.

EXPERIMENTAL RESULTS

Selected backscattered electron (BSE) images of sample cross sections in the system Na_2CO_3-$CaCO_3$ are shown in Figures 3 and 4. The subsolidus samples were represented by homogeneous aggregates of carbonate phases, with grain size varying from several micrometers to several tens of micrometers (Figs. 3a, 3d, 3g, 3j, 4a, 4b, 4d, 4e, 4g, 4j, 4k, and 4l). In non-stoichiometric mixtures, the limiting reagents, i.e., $CaCO_3$ at $X(Na_2CO_3) \geq 30$ mol% (Fig. 3j) and Na_2CO_3 at $X(Na_2CO_3) \leq 60$ mol% (Fig. 3d), have been consumed completely (Table 1). In stoichiometric mixture, $X(Na_2CO_3)$ = 60, 50, and 25 mol%, both reagents, Na_2CO_3 and $CaCO_3$, were completely consumed to form the $Na_2Ca_4(CO_3)_5$ phase after 19 h at 1050 °C (Fig. 4f), while relicts of aragonite and intermediate $Na_2Ca_3(CO_3)_4$ compound remained at 950 °C even after 36 h (Figs. 4d and 4e, Table 1). This suggests that reactions have gone to completion and equilibrium has been achieved in all experiments above 950 °C.

A monophase aggregate of carbonate crystals up to 500 μm in size in the cool region and a melt quenched to a dendritic aggregate and segregated to the hot region were observed in the run products below liquidus (Figs. 3b, 3c, 3e, 3i, 3k, 4h, and 4i). In the case of near eutectic compositions and temperatures, a two-phase aggregate coexisting with liquid was observed (Figs. 3h and 4c). The melts quenched with a rate of about 60 °C/s, were represented by dendritic aggregates rather than glass (Figs. 3b, 3c, 3e, 3h, 3i, 3k, 3l, 4c, 4h, and 4i). Usually, the liquid-crystal interface has a rounded outline coinciding with an ordinary shape of the isotherm in a high-pressure cell (Figs. 3 and 4).

Phase relations established in the system Na_2CO_3-$CaCO_3$ at 6 GPa are illustrated in Figure 5. The system has three intermediate compounds: $Na_4Ca(CO_3)_3$, $Na_2Ca_3(CO_3)_4$, and $Na_2Ca_4(CO_3)_5$. The latter has an upper stability limit between 1050 and 1100 °C, where it undergoes subsolidus breakdown to aragonite and $Na_2Ca_3(CO_3)_4$ according to the reaction: $Na_2Ca_4(CO_3)_5$ = $Na_2Ca_3(CO_3)_4$ + $CaCO_3$ (Figs. 4a and 4b). The distinct liquid compositions at 1200 °C below and above 67 mol% Na_2CO_3 and at 1300 °C below and above 25 mol% Na_2CO_3 suggest a eutectic type phase diagram (Table 1, Fig. 5). This is also supported by a coexistence of liquid with two solid phases in near eutectic compositions at 50 mol% and 1200 °C and 20 mol% and 1300 °C (Figs. 3h and 4c). The topology of the phase diagram implies congruent melting of $Na_4Ca(CO_3)_3$ above 1200 °C and $Na_2Ca_3(CO_3)_4$ above 1300 °C (Fig. 5). The eutectics were established at $X(Na_2CO_3)$ = 70 and 52 mol% near 1200 °C and at $X(Na_2CO_3)$ = 21 mol% near 1300 °C.

The carbonate Na_2CO_3 does not melt up to 1350 °C as it was confirmed in separate run in pure Na_2CO_3 system. Melting of Na_2CO_3 was established at 1400 °C. The established melting temperature is about 500 °C higher than that at ambient pressure (Reisman 1959). Measurable amounts of Ca in Na_2CO_3 suggest an existence of Na_2CO_3 solid solutions at given experimental conditions (Fig. 5, Table 1). The maximum $CaCO_3$ solubility in Na-carbonate of about 6–8 mol% was established in the temperature range of 1100–1300 °C.

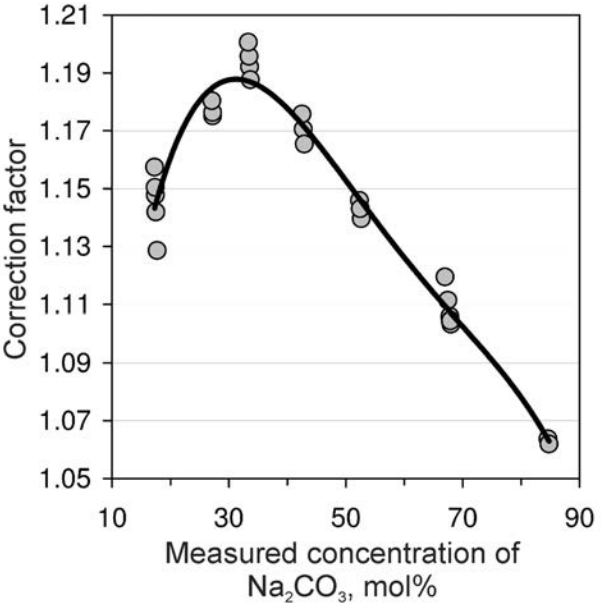

FIGURE 2. EDS correction factor, $k = X_0/X$, vs. measured concentration of Na_2CO_3, X, in mol% for the system Na_2CO_3-$CaCO_3$.

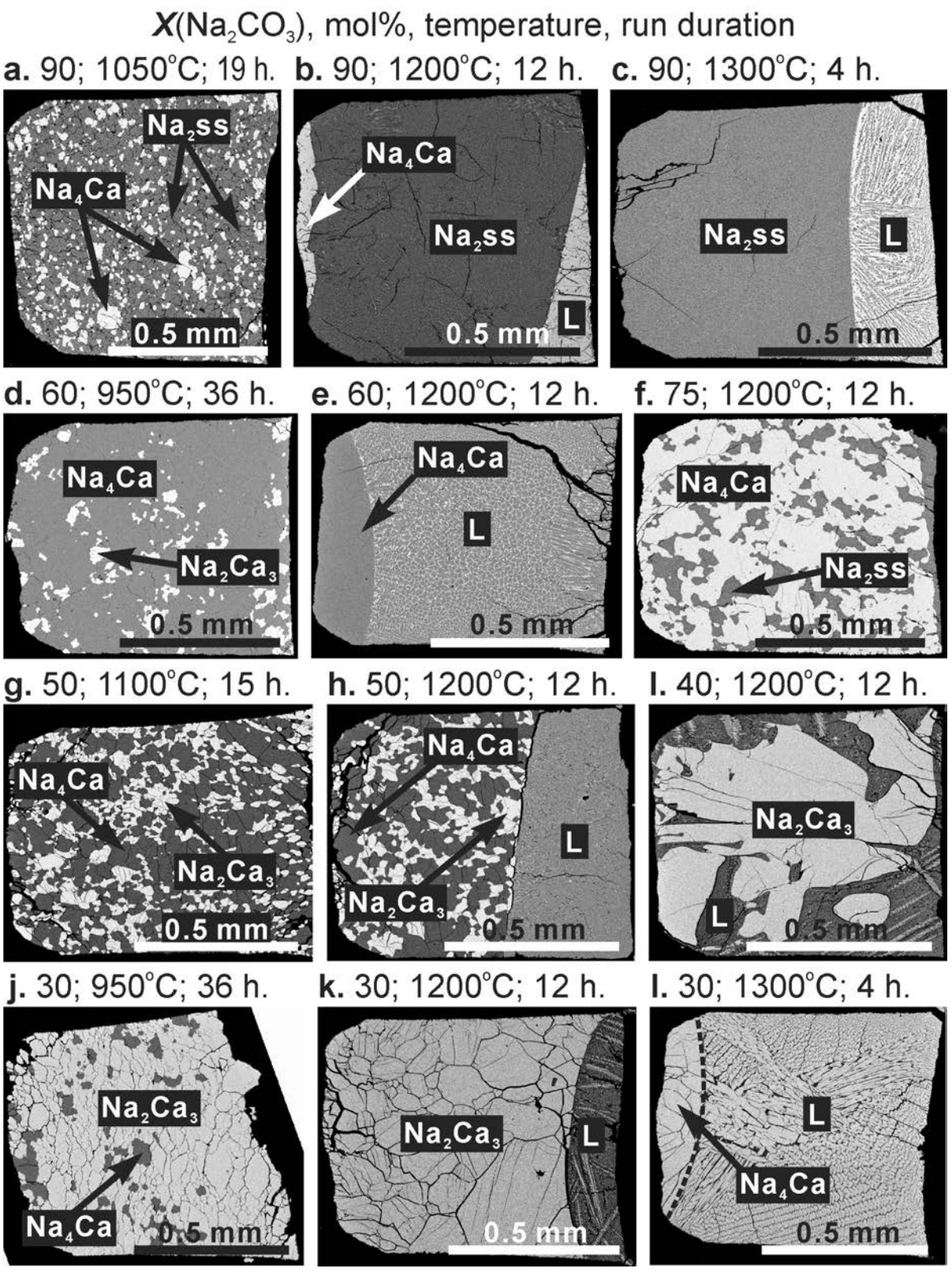

FIGURE 3. Representative BSE images of sample cross sections illustrating phase relations in the system Na_2CO_3-$CaCO_3$ at 6 GPa and $X(Na_2CO_3)$ varying from 90 to 30 mol%. Na_2ss = $CaCO_3$ solid solution in Na_2CO_3; Na_4Ca = $Na_4Ca(CO_3)_3$; Na_2Ca_3 = $Na_2Ca_3(CO_3)_4$; Na_2Ca_4 = $Na_2Ca_4(CO_3)_5$; Art = $CaCO_3$; L = quenched liquid. High-temperature side is located at the right side of each image.

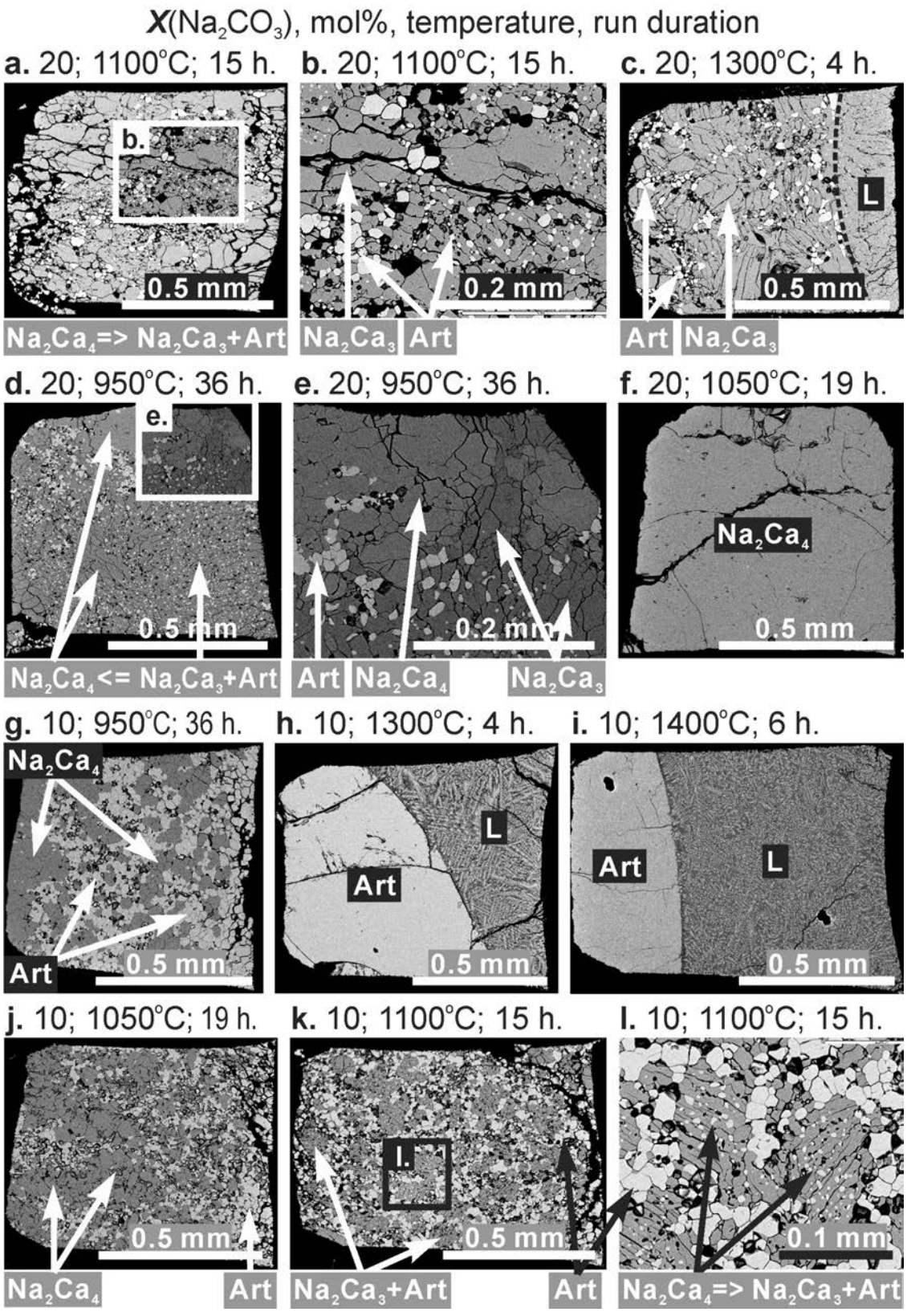

FIGURE 4. Representative BSE images of sample cross sections illustrating phase relations in the system Na_2CO_3-$CaCO_3$ at 6 GPa and $X(Na_2CO_3)$ = 20 and 10 mol%. Legend is the same as in Figure 3.

TABLE 1. Compositions (in mol% Na_2CO_3) of the run products in the system Na_2CO_3-$CaCO_3$ at 6 GPa

Run no.,		*X*(Na_2CO_3) in the system, mol%									
T, time	Phases	90	75	67	60	50	40	30	25	20	10
ES346	Na_2CO_3	–[A]	×	×	×	×	×	–	×	–	–
1400 °C	$CaCO_3$	–	×	×	×	×	×	–	×	–	0.0
6 h	Liquid	+	×	×	×	×	×	+	×	+	16.1(6)
ES344	Na_2CO_3	93.2(2)	–	×	–	–	–	–	×	–	–
1300 °C	$Na_2Ca_3(CO_3)_4$	–	–	×	–	–	–	25.0(2.3)	×	24.9(2.8)	–
4 h	Aragonite	–	–	×	–	–	–	–	×	0.0(3)	0.3
	Liquid	78.6(5)	+	×	+	+	+	31.3(1)	×	21.1(1.8)	20.9(1.8)
T2024	Na_2CO_3	93.1(1.7)	×	×	–	–	×	×	×	×	×
1250 °C	$Na_2Ca_3(CO_3)_4$	–	×	×	–	–	×	×	×	×	×
10 h	Liquid	73.2	×	×	+	+	×	×	×	×	×
ES341	Na_2CO_3	92.3(1)	93.8(4)	×	–	–	–	–	×	–	–
1200 °C	$Na_4Ca(CO_3)_3$	67.9	68.2(1.8)	×	66.0(0)	62.1(1.5)	–	–	×	–	–
12 h	$Na_2Ca_3(CO_3)_4$	–	–	×	–	25.8(2.5)	25.1(2)	26.4(5)	×	24.8(2.8)	25.1(3)
	Aragonite	–	–	×	–	–	–	–	×	0.4(2)	0.3
	Liquid	70.4	–	×	58.7(3)	51.7(3)	50.9(3.8)	50.4(8)	×	–	–
ES352	Na_2CO_3	×	×	×	–	×	×	×	×	–	×
1150 °C	$Na_4Ca(CO_3)_3$	×	×	×	66.1(3)	×	×	×	×	–	×
2.5 h†	$Na_2Ca_3(CO_3)_4$	×	×	×	25.2(6)	×	×	×	×	20.1(3)*	×
T2005	Na_2CO_3	93.9(0)	93.8(1.4)	×	–	–	–	–	×	–	–
1100 °C	$Na_4Ca(CO_3)_3$	68.6	66.9	×	64.7(4)	65.2	64.8	65.0	×	–	–
15 h	$Na_2Ca_3(CO_3)_4$	–	–	×	25.3(2.9)	25.5	24.3(2.7)	25.3	×	25.9	25.7
	Aragonite	–	–	×	–	–	–	–	×	0.1	0.3
ES330	Na_2CO_3	97.3(2)	97.7(3)	×	–	–	–	–	×	–	–
1050 °C	$Na_4Ca(CO_3)_3$	68.7(4)	68.6	×	65.3(3)	66.5(1)	66.3(4)	62.9(9)	×	–	–
19 h	$Na_2Ca_3(CO_3)_4$	–	–	×	26.3(1.5)	25.1(2.5)	25.2(8)	26.0(9)	×	–	–
	$Na_2Ca_4(CO_3)_5$	–	–	×	–	–	–	–	×	20.0(2)	20.8(3)
	Aragonite	–	–		–	–	–	–	×	–	0.0(3)
B1032/1	$Na_4Ca(CO_3)_3$	–	–	67.4(5)	–	–	–	–	–	–	–
1000 °C	$Na_2Ca_3(CO_3)_4$	–	–	–	–	–	–	–	25.8(3)	–	–
30 h											
T2004	Na_2CO_3	99.9(2)	99.6(2)	×	–	–	–	–	×	–	–
950 °C	$Na_4Ca(CO_3)_3$	68.1(4.3)	68.1(3)	×	66.4	65.5(1)	64.5(2)	64.5	×	–	–
36 h	$Na_2Ca_3(CO_3)_4$	–	–	×	26.5(3.1)	25.2(1.1)	25.9(2.5)	25.5(1)	×	25.7(3)	–
	$Na_2Ca_4(CO_3)_5$	–	–	×	–	–	–	–	×	20.7(1)	20.2(6)
	Aragonite	–	–	×	–	–	–	–	×	0.2(0)	0.1(2)
B1000/1	Na_2CO_3	100.0(0)	99.6(2)	×	–	–	–	–	×	–	–
900 °C	$Na_4Ca(CO_3)_3$	67.7(1.9)	67.3(7)	×	65.6(1.6)	66.3(3)	64.8(1)	61.1(9)	×	–	–
38 h	$Na_2Ca_3(CO_3)_4$	–	–	×	27.9(3)	26.2(7)	25.7	26.1(2)	×	25.4	24.7
	$Na_2Ca_4(CO_3)_5$	–	–	×	–	–	–	–	×	–	19.3(2.1)
	Aragonite	–	–	×	–	–	–	–	×	0.1(1)	0.1(2)
				×							
B1032/1	$Na_4Ca(CO_3)_3$	×	×	67.5(4)	×	×	×	×	–	×	×
900 °C	$Na_2Ca_3(CO_3)_4$	×	×	–	×	×	×	×	25.5(4)	×	×
41 h											

Notes: "–" = phase was not established in the run products; "+" = complete melting; × = no data. Standard deviations are given in parentheses, where the number of measurements is more than one. Letters in the run number, ES, T, and B denote the type of multi-anvil apparatus, wedge, DIA and BARS, respectively. [A] = The Na_2CO_3 system.
* The Na_2CO_3(25)-$CaCO_3$(75) system.
† Slow cooling from 1400 to 1150 °C for 2.5 h.

$CaCO_3$, whose melting temperature is about 1700 °C at 6 GPa (Suito et al. 2001), was observed as a subliquidus phase at 1300 °C and *X*($CaCO_3$) > 50 mol% and identified by Raman spectroscopy as aragonite. The Na solubility in aragonite does not exceed the detection limit of EDS employed in our study (i.e., <0.5 mol% Na_2CO_3) (Table 1). Therefore, it is suggested that there is very little, if any, solid solution of Na_2CO_3 in aragonite at 6 GPa.

DISCUSSION

Based on the phase relations in the system Na_2CO_3-$CaCO_3$, we suggest that shortite [$Na_2Ca_2(CO_3)_3$] and nyerereite/zemkorite [$Na_2Ca(CO_3)_2$], the double carbonates observed at 0.1 GPa pressures, are not stable at the pressure conditions of sublithospheric mantle. Moreover, according to our experimental results all Na-Ca carbonates should melt at the temperature conditions of the average mantle adiabat and temperatures expected for ascending kimberlite magma (Kavanagh and Sparks 2009). Therefore, findings of the high-pressure Na-Ca carbonates can hardly be expected in mantle inclusions from kimberlites.

Binary Na-Ca carbonate, shortite, occures in the groundmass of a hypabyssal-facies kimberlites from the Upper Canada Gold Mine, Ontario (Watkinson and Chao 1973), Venkatampalle, Andhra Pradesh, India (Parthasarathy et al. 2002), and Udachnaya-East pipe, Yakutia, Russia (Yegorov et al. 1988). Cooper and Gittins (1974) interpreted them as products of the subsolidus breakdown of nyerereite, which precipitated from residual liquid during crystallization of kimberlite magma. The Udachnaya occurrence is extremely interesting because of its implications regarding the nature of magma involved in the kimberlite emplacement and possible relation to the alkali-rich carbonatite magma. For instance, abundant carbonates (calcite, zemkorite/nyerereite and shortite, up to 30 vol%) in the groundmass assemblage of Udachnaya-East kimberlite resemble

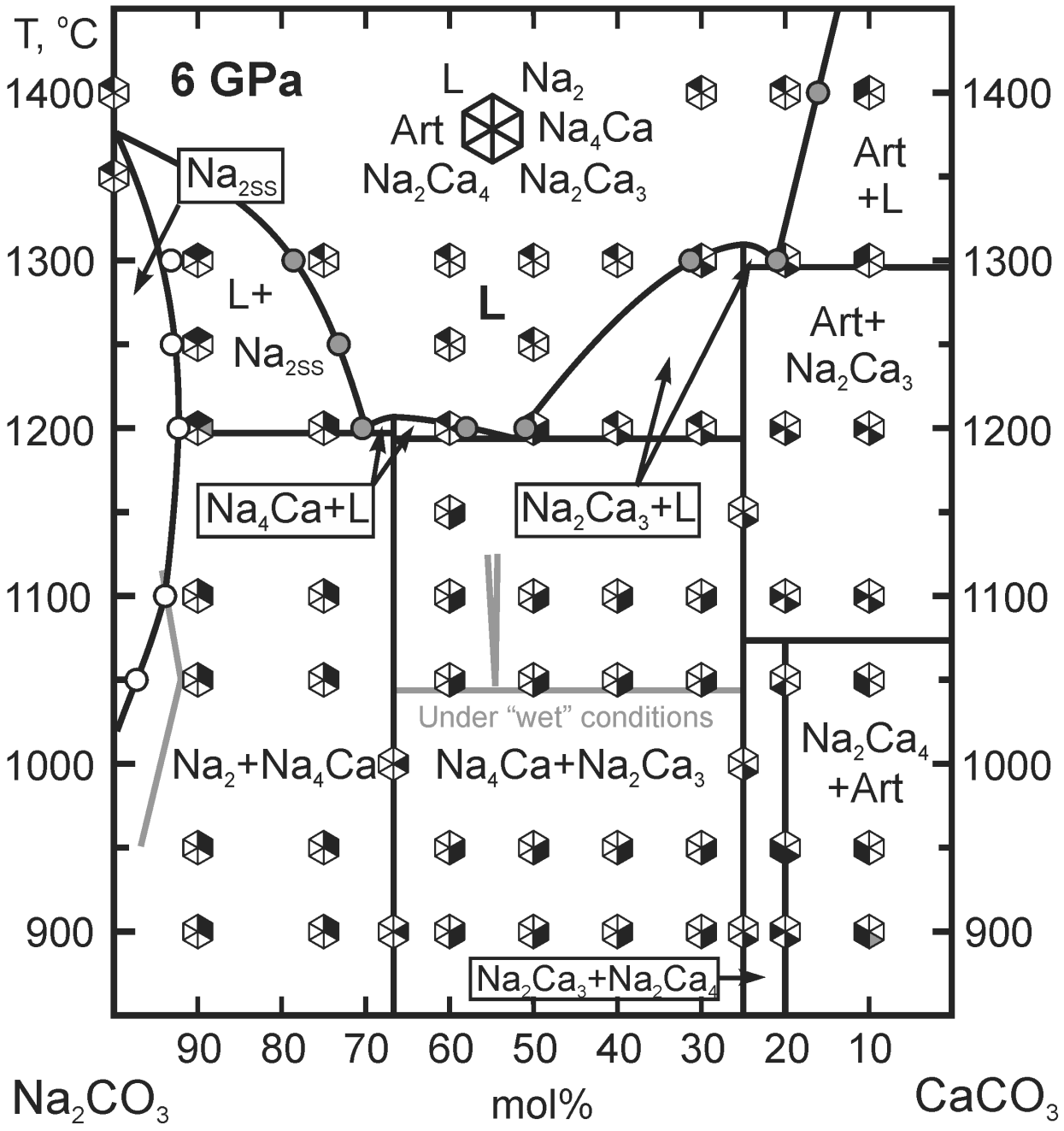

FIGURE 5. Phase relations in Na_2CO_3-$CaCO_3$ system at 6 GPa. $Na_2 = Na_2CO_3$; $Na_{2SS} = CaCO_3$ solid-solution in Na_2CO_3; $Na_4Ca = Na_4Ca(CO_3)_3$; $Na_2Ca_3 = Na_2Ca_3(CO_3)_4$; $Na_2Ca_4 = Na_2Ca_4(CO_3)_5$; Art = $CaCO_3$; L = liquid. Gray circles indicate melt composition measured by EDS. White circles mark composition of Na_2CO_3 solid solution. Insufficient sample drying (at 100 °C instead of 300 °C) lowers Na_4Ca-Na_2Ca_3 eutectic temperature to 1150 °C and expands the Na_2CO_3 solid-solution field at lower temperature (gray lines). The gray-hatched area at 900 °C and $X(Na_2CO_3)$ = 10 mol% bulk composition marks the presence of relicts of the intermediate $Na_2Ca_3(CO_3)_4$ compound. The gray-hatched area at 1200 °C and $X(Na_2CO_3)$ = 90 mol% bulk composition marks the presence of $Na_4Ca(CO_3)_3$ in the cool region.

modern natrocarbonatite lavas from Oldoinyo Lengai volcano (Kamenetsky et al. 2007). As follows from experimentally obtained phase diagram (3–6.5 GPa, 900–1500 °C) of Udachnaya-East kimberlite, the proto-kimberlitic magma, which originates from more than 220 km depth (Agashev et al. 2008), was essentially Na-Ca-carbonatite melt [≤15 wt% SiO_2, Na_2O+K_2O = 5–18 wt%, Na/K≈2, Ca/(Ca+Mg+Fe) = 0.6–0.8] (Sharygin et al. 2013). Possible existence of Na-rich carbonatite precursor of kimberlite magma was also assumed to explain formation of "$En_{40}Di_{20}Jd_{40}$" and "NaPxEn" inclusions in diamonds (Gasparik

and Hutchison 2000) and confirmed by direct findings of Na-Ca carbonate-bearing melt inclusions, which may have originated in the lower mantle and/or transition zone (Kaminsky et al. 2009).

Implications

The present results suggest that possible Na-bearing phases in the H_2O-poor carbonated mantle are sodium-calcium carbonates $Na_2Ca_3(CO_3)_4$ and $Na_2Ca_4(CO_3)_5$. Eutectic temperature of the $Na_2Ca_3(CO_3)_4$-$CaCO_3$ join is between the 40 and 45 mW/m^2 geotherms of Pollack and Chapman (1977) at 6 GPa. This means that Na-rich carbonated mantle rocks will produce carbonate melts even at a relatively cold cratonic geotherm. Yet, under these conditions sodium tends to dissolves into clinopyroxene structure as $NaAlSi_2O_6$, rather than into carbonates (Grassi and Schmidt 2011). Consequently, the stability of Na-Ca carbonates would be restricted by the alumina-depleted ultramafic compositions such as carbonated-dunite or harzburgite. Once $Na_2Ca_3(CO_3)_4$ is a stable subsolidus phase, it could play a major role in controlling both the temperature of melting and the composition of the melt produced.

Acknowledgments

We thank W. Crichton, S. Keshav, and R. Dasgupta for thorough reviews and suggestions and J. Kung for editorial handling and comments. This study was conducted as a part of the Global Center-of-Excellence program at Tohoku University. This work was also supported by the Ministry of education and science of Russia (Project Nos. 14.B37.21.0601 and 14.B25.31.0032) and the Russian Foundation for Basic Research (Project Nos. 12-05-01167 and 12-05-33008).

References cited

Agashev, A.M., Pokhilenko, N.R., Takazawa, E., McDonald, J.A., Vavilov, M.A., Watanabe, I., and Sobolev, N.V. (2008) Primary melting sequence of a deep (>250 km) lithospheric mantle as recorded in the geochemistry of kimberlite-carbonatite assemblages, Snap Lake dyke system, Canada. Chemical Geology, 255, 317–328.

Akaishi, M., Kanda, H., and Yamaoka, S. (1990) Synthesis of diamond from graphite-carbonate systems under very high temperature and pressure. Journal of Crystal Growth, 104, 578–581.

Brey, G.P., Bulatov, V.K., and Girnis, A.V. (2011) Melting of K-rich carbonated peridotite at 6-10 GPa and the stability of K-phases in the upper mantle. Chemical Geology, 281, 333–342.

Buob, A., Luth, R.W., Schmidt, M.W., and Ulmer, P. (2006) Experiments on $CaCO_3$-$MgCO_3$ solid solutions at high pressure and temperature. American Mineralogist, 91, 435–440.

Cooper, A.F., and Gittins, J. (1974) Shortite in kimberlite from the Upper Canada Gold mine: a discussion. Journal of Geology, 82, 667–669.

Cooper, A.F., Gittins, J., and Tuttle, O.F. (1975) The system Na_2CO_3-K_2CO_3-$CaCO_3$ at 1 kilobar and its significance in carbonatite petrogenesis. American Journal of Science, 275, 534–560.

Dalton, J.A., and Presnall, D.C. (1998) The continuum of primary carbonatitic-kimberlitic melt compositions in equilibrium with lherzolite: Data from the system CaO-MgO-Al2O3-SiO2-CO2 at 6 GPa. Journal of Petrology, 39, 1953–1964.

Dasgupta, R., and Hirschmann, M.M. (2006) Melting in the Earth's deep upper mantle caused by carbon dioxide. Nature, 440, 659–662.

Dasgupta, R., Mallik, A., Tsuno, K., Withers, A.C., Hirth, G., and Hirschmann, M.M. (2013) Carbon-dioxide-rich silicate melt in the Earth's upper mantle. Nature, 493, 211–222.

Dawson, J.B. (1962) Sodium carbonate lavas from Oldoinyo Lengai, Tanganyika. Nature, 195, 1075–1076.

Eitel, W., and Skaliks, W. (1929) Some double carbonates of alkali and earth alkali. Zeitschrift Für Anorganische Und Allgemeine Chemie, 183, 263–286.

Gasparik, T., and Hutchison, M.T. (2000) Experimental evidence for the origin of two kinds of inclusions in diamonds from the deep mantle. Earth and Planetary Science Letters, 181, 103–114.

Golovin, A.V., Sharygin, I.S., Korsakov, A.V., and Pokhilenko, N.P. (2012) Can parental kimberlite melts be alkali-carbonate liquids: Results of investigation of composition melt inclusions in the mantle xenoliths from kimberlites. 10th International Kimberlite Conference, p. 10IKC-91, Bangalore, India.

Grassi, D., and Schmidt, M.W. (2011) The melting of carbonated pelites from 70 to 700 km depth. Journal of Petrology, 52, 765–789.

Green, D.H., and Wallace, M.E. (1988) Mantle metasomatism by ephemeral carbonatite melts. Nature, 336, 459–462.

Haggerty, S.E. (1989) Mantle metasomes and the kinship between carbonatites and kimberlites. In K. Bell, Ed., Carbonatites: Genesis and Evolution, p. 546–560. Unwin Hyman, London.

Hay, R.L. (1983) Natrocarbonatite tephra of Kerimasi volcano, Tanzania. Geology, 11, 599–602.

Kamenetsky, M.B., Sobolev, A.V., Kamenetsky, V.S., Maas, R., Danyushevsky, L.V., Thomas, R., Pokhilenko, N.P., and Sobolev, N.V. (2004) Kimberlite melts rich in alkali chlorides and carbonates: A potent metasomatic agent in the mantle. Geology, 32, 845–848.

Kamenetsky, V.S., Kamenetsky, M.B., Sharygin, V.V., and Golovin, A.V. (2007) Carbonate-chloride enrichment in fresh kimberlites of the Udachnaya-East pipe, Siberia: A clue to physical properties of kimberlite magmas? Geophysical Research Letters, 34, L09316.

Kamenetsky, V.S., Kamenetsky, M.B., Weiss, Y., Navon, O., Nielsen, T.F.D., and Mernagh, T.P. (2009) How unique is the Udachnaya-East kimberlite? Comparison with kimberlites from the Slave Craton (Canada) and SW Greenland. Lithos, 112, 334–346.

Kamenetsky, V.S., Grutter, H., Kamenetsky, M.B., and Gomann, K. (2012) Parental carbonatitic melt of the Koala kimberlite (Canada): Constraints from melt inclusions in olivine and Cr-spinel, and groundmass carbonate. Chemical Geology, 353, 96–111, http://dx.doi.org/10.1016/j.chemgeo.2012.09.022.

Kaminsky, F., Wirth, R., Matsyuk, S., Schreiber, A., and Thomas, R. (2009) Nyerereite and nahcolite inclusions in diamond: evidence for lower-mantle carbonatitic magmas. Mineralogical Magazine, 73, 797–816.

Kanda, H., Akaishi, M., and Yamaoka, S. (1990) Morphology of synthetic diamonds grown from Na_2CO_3 solvent-catalyst. Journal of Crystal Growth, 106, 471–475.

Kavanagh, J.L., and Sparks, R.S.J. (2009) Temperature changes in ascending kimberlite magma. Earth and Planetary Science Letters, 286, 404–413.

Klein-BenDavid, O., Izraeli, E.S., Hauri, E., and Navon, O. (2004) Mantle fluid evolution—A tale of one diamond. Lithos, 77, 243–253.

——— (2007) Fluid inclusions in diamonds from the Diavik mine, Canada and the evolution of diamond-forming fluids. Geochimica et Cosmochimica Acta, 71, 723–744.

Klein-BenDavid, O., Logvinova, A.M., Schrauder, M., Spetius, Z.V., Weiss, Y., Hauri, E.H., Kaminsky, F.V., Sobolev, N.V., and Navon, O. (2009) High-Mg carbonatitic microinclusions in some Yakutian diamonds—A new type of diamond-forming fluid. Lithos, 112, 648–659.

Korsakov, A.V., Golovin, A.V., De Gussem, K., Sharygin, I.S., and Vandenabeele, P. (2009) First finding of burkeite in melt inclusions in olivine from sheared lherzolite xenoliths. Spectrochimica Acta Part A: Molecular and Biomolecular Spectroscopy, 73, 424–427.

Litasov, K.D., and Ohtani, E. (2009) Solidus and phase relations of carbonated peridotite in the system CaO-Al_2O_3-MgO-SiO_2-Na_2O-CO_2 to the lower mantle depths. Physics of the Earth and Planetary Interiors, 177, 46–58.

——— (2010) The solidus of carbonated eclogite in the system CaO-Al_2O_3-MgO-SiO_2-Na_2O-CO_2 to 32 GPa and carbonatite liquid in the deep mantle. Earth and Planetary Science Letters, 295, 115–126.

Litasov, K.D., Shatskiy, A., Ohtani, E., and Yaxley, G.M. (2013) The solidus of alkaline carbonatite in the deep mantle. Geology, 41, 79–82.

Logvinova, A.M., Wirth, R., Tomilenko, A.A., Afanas'ev, V.P., and Sobolev, N.V. (2011) The phase composition of crystal-fluid nanoinclusions in alluvial diamonds in the northeastern Siberian Platform. Russian Geology and Geophysics, 52, 1286–1297.

Merlini, M., Crichton, W.A., Hanfland, M., Gemmi, M., Muller, H., Kupenko, I., and Dubrovinsky, L. (2012a) Structures of dolomite at ultrahigh pressure and their influence on the deep carbon cycle. Proceedings of the National Academy of Sciences, 109, 13509–13514.

Merlini, M., Hanfland, M., and Crichton, W.A. (2012b) $CaCO_3$-III and $CaCO_3$-VI, high-pressure polymorphs of calcite: Possible host structures for carbon in the Earth's mantle. Earth and Planetary Science Letters, 333–334, 265–271.

Navon, O. (1991) High internal pressure in diamond fluid inclusions determined by infrared absorption. Nature, 353, 746–748.

Ono, S., Kikegawa, T., Ohishi, Y., and Tsuchiya, J. (2005) Post-aragonite phase transformation in $CaCO_3$ at 40 GPa. American Mineralogist, 90, 667–671.

Ono, S., Kikegawa, T., and Ohishi, Y. (2007) High-pressure transition of $CaCO_3$. American Mineralogist, 92, 1246–1249.

Pal'yanov, Y.N., Sokol, A.G., Borzdov, Y.M., Khokhryakov, A.F., and Sobolev, N.V. (1999) Diamond formation from mantle carbonate fluids. Nature, 400, 417–418.

Pal'yanov, Y.N., Sokol, A.G., Borzdov, Y.M., and Khokhryakov, A.F. (2002) Fluid-bearing alkaline carbonate melts as the medium for the formation of diamonds in the Earth's mantle: an experimental study. Lithos, 60, 145–159.

Palyanov, Y.N., Borzdov, Y.M., Khokhryakov, A.F., Kupriyanov, I.N., and Sokol, A.G. (2010) Effect of nitrogen impurity on diamond crystal growth processes. Crystal Growth & Design, 10, 3169–3175.

Palyanov, Y.N., Shatsky, V.S., Sobolev, N.V., and Sokol, A.G. (2007) The role of mantle ultrapotassic fluids in diamond formation. Proceedings of the National

Academy of Sciences, 104, 9122–9127.
Parthasarathy, G., Chetty, T.R.K., and Haggerty, S.E. (2002) Thermal stability and spectroscopic studies of zemkorite: A carbonate from the Venkatampalle kimberlite of southern India. American Mineralogist, 87, 1384–1389.
Pollack, H.N., and Chapman, D.S. (1977) On the regional variation of heat flow, geotherms, and lithospheric thickness. Tectonophysics, 38, 279–296.
Reisman, A. (1959) Heterogeneous equilibria in the system K_2CO_3-Na_2CO_3. Journal of the American Chemical Society, 81, 807–811.
Schrauder, M., and Navon, O. (1994) Hydrous and carbonatitic mantle fluids in fibrous diamonds from Jwaneng, Botswana. Geochimica et Cosmochimica Acta, 58, 761–771.
Sharygin, I.S., Litasov, K.D., Shatskiy, A.F., Golovin, A.V., Ohtani, E., and Pokhilenko, N.P. (2013) Melting of kimberlite of the Udachnaya East pipe: experimental study at 3–6.5 GPa and 900–1500°C. Doklady Earth Sciences, 448, 200–205.
Shatskii, A.F., Borzdov, Y.M., Sokol, A.G., and Pal'yanov, Y.N. (2002) Phase formation and diamond crystallization in carbon-bearing ultrapotassic carbonate-silicate systems. Geologiya I Geofizika, 43, 940–950.
Shatskiy, A., Borzdov, Y.M., Litasov, K.D., Ohtani, E., Khokhryakov, A.F., Palyanov, Y.N., and Katsura, T. (2011a) Pressless split-sphere apparatus equipped with scaled-up Kawai-cell for mineralogical studies at 10–20 GPa. American Mineralogist, 96, 541–548.
Shatskiy, A., Katsura, T., Litasov, K.D., Shcherbakova, A.V., Borzdov, Y.M., Yamazaki, D., Yoneda, A., Ohtani, E., and Ito, E. (2011b) High pressure generation using scaled-up Kawai-cell. Physics of the Earth and Planetary Interiors, 189, 92–108.
Shatskiy, A., Sharygin, I.S., Gavryushkin, P.N., Litasov, K.D., Borzdov, Y.M., Shcherbakova, A.V., Higo, Y., and Funakoshi, K. (2013) The system K_2CO_3-$MgCO_3$ at 6 GPa and 900–1450 °C. American Mineralogist, 98, 1593–1603.
Spivak, A.V., Litvin, Y.A., Ovsyannikov, S.V., Dubrovinskaia, N.A., and Dubrovinsky, L.S. (2012) Stability and breakdown of $Ca^{13}CO_3$ melt associated with formation of ^{13}C-diamond in static high pressure experiments up to 43 GPa and 3900 K. Journal of Solid State Chemistry, 191, 102–106.
Suito, K., Namba, J., Horikawa, T., Taniguchi, Y., Sakurai, N., Kobayashi, M., Onodera, A., Shimomura, O., and Kikegawa, T. (2001) Phase relations of $CaCO_3$ at high pressure and high temperature. American Mineralogist, 86, 997–1002.
Wallace, M.E., and Green, D.H. (1988) An experimental determination of primary carbonatite magma composition. Nature, 335, 343–346.
Walter, M.J., Bulanova, G.P., Armstrong, L.S., Keshav, S., Blundy, J.D., Gudfinnsson, G., Lord, O.T., Lennie, A.R., Clark, S.M., Smith, C.B., and Gobbo, L. (2008) Primary carbonatite melt from deeply subducted oceanic crust. Nature, 454, 622–630.
Watkinson, D.H., and Chao, G.Y. (1973) Shortite in kimberlite from Upper Canada gold mine, Ontario. Journal of Geology, 81, 229–233.
Weiss, Y., Kessel, R., Griffin, W.L., Kiflawi, I., Klein-BenDavid, O., Bell, D.R., Harris, J.W., and Navon, O. (2009) A new model for the evolution of diamond-forming fluids: Evidence from microinclusion-bearing diamonds from Kankan, Guinea. Lithos, 112, 660–674.
Wyllie, P.J., and Huang, W.L. (1975) Peridotite, kimberlite, and carbonatite explained in the system CaO-MgO-SiO_2-CO_2. Geology, 3, 621–624.
Yaxley, G.M., Crawford, A.J., and Green, D.H. (1991) Evidence for carbonatite metasomatism in spinel peridotite xenoliths from western Victoria, Australia. Earth and Planetary Science Letters, 107, 305–317.
Yegorov, N.K., Ushchapovskaya, Z.F., Kashyev, A.A., Bogdanov, G.V., and Sizykh, Y.I. (1988) Zemkorite, a new carbonate from kimberlites of Yakutia. Doklady Akademii Nauk SSSR, 30, 188–193.
Zaitsev, A.N., and Keller, J. (2006) Mineralogical and chemical transformation of Oldoinyo Lengai natrocarbonatites, Tanzania. Lithos, 91, 191–207.
Zedgenizov, D.A., Ragozin, A.L., Shatsky, V.S., Araujo, D., and Griffin, W.L. (2011) Fibrous diamonds from the placers of the northeastern Siberian Platform: carbonate and silicate crystallization media. Russian Geology and Geophysics, 52, 1298–1309.

Manuscript received December 11, 2012
Manuscript accepted July 2, 2013
Manuscript handled by Jennifer Kung